

Introduction

Knowledge of the sensitivity of a solution to small changes in the model parameters is exploited in many areas in computational physics and used to perform mesh adaptivity (Power et al., 2006), or to correct errors based on discretisation and sub-grid-scale modelling (Merton et al., 2013, 2014), to perform the assimilation of data based on adjusting the most sensitive parameters to the model-observation misfit, and similarly to form optimised sub-grid-scale models (Cacuci et al., 2005; Maday and Taddei, 2017; Shah, 2017; Liu and Kalnay, 2008; Hossen et al., 2012). We present a goal-based approach for forming sensitivity (or importance) maps using ensembles. These maps are defined as regions in space and time of high relevance for a given goal, for example, the solution at an observation point within the domain. The presented approach relies solely on ensembles obtained from the forward model and thus can be used with complex models for which calculating an adjoint (Ionescu-Bujor and Cacuci, 2004; Wang et al., 1992; Cacuci, 2015) is not a practical option. This provides a simple approach for optimisation of sensor placement, goal based mesh adaptivity, assessment of goals and data assimilation. We investigate methods which reduce the number of ensembles used to construct the maps yet which retain reasonable fidelity of the maps.

The fidelity comes from an integrated method including a goal-based approach, in which the most up-to-date importance maps are fed back into the perturbations to focus the algorithm on the key variables and domain areas. Also within the method smoothing (Blum et al., 2009; Nerger et al., 2014; Attia, 2016) is applied to the perturbations to obtain a multi-scale, global picture of the sensitivities; the perturbations are orthogonalised (Attia, 2016; Leroux et al., 2018; Keller et al., 2010; Che et al., 2014) inverted; and time windows (Attia, 2016) are applied (for time dependent problems) where we work backwards in time to obtain greater accuracy of the sensitivity maps.

The theory section describes the background to our ensemble-based approach as well as outlining some recent developments which we test on a porous media multi-phase flow problem in the results section of this paper. We finish by drawing conclusions.

Theory

This paper describes a method of calculating the sensitivity of a functional with respect to the solution based on an ensemble method.

We begin the theory section by showing how changes in the controls (problem parameters or inputs) or the solutions affect the value of a functional (*Calculating sensitivities*). We demonstrate how ensembles can approximate sensitivities in a steady-state setting (*Forming sensitivities by using ensembles*) and then extend this to a time-dependent situations (*Time dependent problems*). Finally, we outline a novel approach developed in Heaney et al. (2018) (*Goal-based weighting of perturbations, Time windows*).

Calculating sensitivities

Suppose we have inputs, $\bar{\mathbf{m}}$, for a computational model, and the corresponding outputs: the solution, $\bar{\boldsymbol{\psi}}$, and a quantity of interest encapsulated by a functional of value \bar{F} . We refer to these as unperturbed quantities. Now we choose to run a similar problem but with slightly different inputs, \mathbf{m} , producing results $\boldsymbol{\psi}$ and F . These quantities are related to the previous, unperturbed quantities by the following

$$\mathbf{m} = \bar{\mathbf{m}} + \Delta\mathbf{m}, \quad (1)$$

$$\boldsymbol{\psi} = \bar{\boldsymbol{\psi}} + \Delta\boldsymbol{\psi}, \quad (2)$$

$$F = \bar{F} + \Delta F, \quad (3)$$

where $\Delta\mathbf{m}$ are the perturbations made to the input controls, and $\Delta\boldsymbol{\psi}$ and ΔF are the changes resulting from this perturbation which occur in the solution and the functional respectively.

The influence that changing the controls has on the solution and the functional can be approximated as a pair of first order Taylor series expansions

$$\Delta\boldsymbol{\psi} = \mathbf{M}\Delta\mathbf{m} \quad (4)$$

$$\Delta F = \Delta\mathbf{m}^T \frac{dF}{d\mathbf{m}}, \quad (5)$$

where

$$\mathbf{M} = \frac{d\boldsymbol{\psi}}{d\mathbf{m}} \quad \text{and} \quad F = F(\boldsymbol{\psi}(\mathbf{m}), \mathbf{m}). \quad (6)$$

We wish to combine these expressions to come up with a relationship describing how a change in the solution affects the functional. In order to obtain an expression for $\Delta \mathbf{m}$ in terms of $\Delta \boldsymbol{\psi}$ we apply the Moore-Penrose pseudo-inverse to equation (4) which gives

$$\Delta \mathbf{m} = (\mathbf{M}^T \mathbf{M})^{-1} \mathbf{M}^T \Delta \boldsymbol{\psi}. \quad (7)$$

After substituting this into equation (5) we have

$$\Delta F = \Delta \boldsymbol{\psi}^T \left(\mathbf{M} (\mathbf{M}^T \mathbf{M})^{-1} \frac{dF}{d\mathbf{m}} \right) =: \Delta \boldsymbol{\psi}^T \mathbf{g}. \quad (8)$$

We define \mathbf{g} to be the relationship between a change in the solution and a change in the functional. From equation (8), we can see that the term in brackets, \mathbf{g} , is the total derivative of the functional with respect to the solution variables, that is

$$\mathbf{g} \equiv \frac{dF}{d\boldsymbol{\psi}}. \quad (9)$$

Hence, \mathbf{g} is equivalent to the functional's sensitivity with respect to the solution. From this point onwards, \mathbf{g} is referred to as a sensitivity map.

Forming sensitivities by using ensembles

In the previous section we used an ensemble of size one, i.e. there was one set of inputs and outputs from an unperturbed model, and another set of inputs and outputs derived from perturbed controls. We now consider the general case of an ensemble size of \mathcal{E} . Each member of the ensemble has its own perturbed controls, written as ${}^e \mathbf{m}$, which satisfy ${}^e \mathbf{m} = \bar{\mathbf{m}} + \Delta {}^e \mathbf{m}$. Here e represents the ensemble index. We can now study the sensitivity of the functional to the solution in an ensemble-based setting.

First, however, we make a change of variables to map the controls into a space where there is a reduced number of variables. To this end, we introduce a second set of control variables $\Delta {}^e \mathbf{m}_s$. The number of entries in this vector is equal to the ensemble size, \mathcal{E} . The values of the entries are either zero or one:

$$(\Delta {}^e \mathbf{m}_s)_k = \begin{cases} 0 & \text{for } k \in \{1, \dots, \mathcal{E}\}, k \neq e \\ 1 & \text{for } k = e. \end{cases} \quad (10)$$

The relationship between $\Delta {}^e \mathbf{m}_s$ and $\Delta {}^e \mathbf{m}$ is given by

$$\mathbf{C} \Delta {}^e \mathbf{m}_s = \Delta {}^e \mathbf{m} \quad \forall e, \quad (11)$$

where $\mathbf{C}_{ie} = \Delta {}^e \mathbf{m}_i$. Performing a sensitivity analysis with the new variables means that we have the following in place of equation (8)

$$\Delta F = \Delta \mathbf{m}_s^T \frac{dF}{d\mathbf{m}_s} = \Delta \boldsymbol{\psi}^T \left(\mathbf{M}_s (\mathbf{M}_s^T \mathbf{M}_s)^{-1} \frac{dF}{d\mathbf{m}_s} \right) = \Delta \boldsymbol{\psi}^T \mathbf{g}. \quad (12)$$

While the size of the matrix \mathbf{M} was \mathcal{N} by \mathcal{C} (where \mathcal{C} is the number of controls), the size of the matrix \mathbf{M}_s is \mathcal{N} by \mathcal{E} . This change of variables has been advantageous because, for our applications, $\mathcal{E} \ll \mathcal{C}$.

We must estimate \mathbf{M}_s and $dF/d\mathbf{m}_s$ if we wish to be able to calculate the sensitivity map (see equation (12)). The change of variables sets the perturbation size to be 1, which means we can make the following estimations:

$$\frac{dF}{d\mathbf{m}_s} \approx \frac{\widehat{dF}}{d\mathbf{m}_s} = ({}^1 F - \bar{F}, {}^2 F - \bar{F}, \dots, {}^{\mathcal{E}} F - \bar{F})^T \quad (13)$$

$$\mathbf{M}_s = \frac{d\boldsymbol{\psi}}{d\mathbf{m}_s} \approx \widehat{\mathbf{M}}_s = ({}^1 \boldsymbol{\psi} - \bar{\boldsymbol{\psi}}, {}^2 \boldsymbol{\psi} - \bar{\boldsymbol{\psi}}, \dots, {}^{\mathcal{E}} \boldsymbol{\psi} - \bar{\boldsymbol{\psi}}). \quad (14)$$

We insert these estimations into equation (12) and obtain

$$\widehat{\Delta F} = \widehat{\Delta \boldsymbol{\psi}}^T \left(\widehat{\mathbf{M}}_s (\widehat{\mathbf{M}}_s^T \widehat{\mathbf{M}}_s)^{-1} \frac{\widehat{dF}}{d\mathbf{m}_s} \right) = \widehat{\Delta \boldsymbol{\psi}}^T \widehat{\mathbf{g}}, \quad (15)$$

where $\widehat{\Delta F} \approx \Delta F$, $\widehat{\Delta \psi} \approx \Delta \psi$ and $\widehat{\mathbf{g}} \approx \mathbf{g}$.

Another advantage of the change of variables is that neither $dF/d\mathbf{m}_s$ nor $\widehat{\mathbf{M}}_s$ are influenced by the controls, \mathbf{m}_s , because ψ and F are also not influenced by \mathbf{m}_s , see equations (13) and (14). As a result the sensitivity map does not depend on the matrix \mathbf{C} so we never have to construct this matrix. The inversion of the matrix $\widehat{\mathbf{M}}_s^T \widehat{\mathbf{M}}_s$, which is needed to calculate $\widehat{\mathbf{g}}$, will also be realistic as its dimensions are the same as the number of ensemble members used, \mathcal{E} .

Time dependent problems

In order to decouple in time so we can solve for the sensitivity at each time level independently, we apply the change of variables to equation (10) and the approximations given in equations (13), (14) and following (15), which gives

$$\widehat{\Delta \psi} = \widehat{\mathbf{M}}_s \Delta \mathbf{m}_s. \quad (16)$$

where, in full,

$$\left((\widehat{\Delta \psi}^1)^T, \dots, (\widehat{\Delta \psi}^{\mathcal{N}_t})^T \right)^T = \left((\widehat{\mathbf{M}}_s^1)^T, \dots, (\widehat{\mathbf{M}}_s^{\mathcal{N}_t})^T \right)^T \Delta \mathbf{m}_s. \quad (17)$$

In the above, we denote the time level by a superscript and the number of time levels is given by \mathcal{N}_t . The system of equations (17) can now be decoupled in time and, once the Moore-Penrose pseudo-inverse is applied to the equation for each time level in turn, we have

$$\widehat{\mathbf{g}}^n = \widehat{\mathbf{M}}_s^n \left((\widehat{\mathbf{M}}_s^n)^T \widehat{\mathbf{M}}_s^n \right)^{-1} \frac{dF}{d\mathbf{m}_s^n}, \quad (18)$$

for time level n . For more information, see Heaney et al. (2018).

We now describe two novel contributions to ensemble generation: using the sensitivity map to weight the perturbations and the introduction of time windows Heaney et al. (2018).

Goal-based weighting of the perturbations

Goal-based mesh adaptivity Power et al. (2006), and goal-based sensor optimisation methods Che et al. (2014), share some similarities with this approach, however, the method described here will focus perturbations over the regions of interest rather than refine a mesh or observations over a region.

Closer inspection of equation (15) indicates that each contribution to $\widehat{\Delta F}$ takes the following form

$$\widehat{\Delta \psi}_i \widehat{\mathbf{g}}_i. \quad (19)$$

The importance to the functional of the i^{th} solution variable is determined by the value of the i^{th} entry of the sensitivity map. When $\widehat{\mathbf{g}}$ is close to zero, there will, therefore, be little gained by perturbing the controls there. Concentrating the perturbations by weighting them from the sensitivity map was motivated by equation (19). In doing this, we produce perturbations which will have the greatest effect on the functional.

We now derive an expression for the goal-based weighting of the perturbations. The current value of $\widehat{\mathbf{g}}^0$ (the sensitivity map at at time level zero) can be used to concentrate the perturbations in the areas that are of more significance to the goal of the particular problem:

$$\Delta \mathbf{m}_i \rightarrow \frac{|\widehat{\mathbf{g}}_i^0| \Delta \mathbf{m}_i}{\|\widehat{\mathbf{g}}^0\|_\infty}, \quad (20)$$

where i is the node or control volume index and $\|\cdot\|_\infty$ represents is the Euclidean norm. (We do not invoke the Einstein convention for the repeated index.)

Alongside the goal-based weighting, we use three well-known techniques when generating ensembles: random perturbations, smoothing and orthogonalisation. Random perturbations will excite all solution modes simultaneously. Using this approach, instead of perturbing each degree of freedom one-by-one, can produce good results for smaller ensemble sizes. We also smooth the perturbations to lose noise on the grid-scale Shapiro (1970). Larger-scale structures are identified by the smoothed perturbations,

and this will also reduce the size of ensemble required. Finally, we apply the standard Gram-Schmidt orthogonalisation to successive perturbations to ensure that the system is well posed.

Our recipe for generating ensemble perturbations is a combination of the above techniques:

- generate uniformly distributed random perturbations
- smooth the perturbations
- use the most recent sensitivity map to focus the perturbations
- apply Gram-Schmidt orthogonalisation

The modified perturbations are then added to the unperturbed initial conditions and the forward model is run so we obtain the solution and the functional value. On the following page we give a more detailed view of the whole algorithm for a time-dependent problem in Algorithm 1.

Time windows

For some time-dependent applications, it can be useful to split up the time domain into ‘time windows’ and apply the approach described here to each window in turn (starting with the last one chronologically and working backwards in time). The perturbations can then be tailored for the physics in each time window by the algorithm. If required, information can be passed back from one time window to another by using the matrix $\widehat{\mathbf{M}}_s^n$. For more details see Heaney et al. (2018).

This approach has similarities with adjoint methods which send back in time information from the functional to discover which are the variables that influence the functional and how much they do so.

The time windows, goal-based weighting, use of random perturbations, smoothing and orthogonalisation all contribute to the reduction of ensemble size required to attain a ‘reasonably’ accurate sensitivity map and thus the computational efficiency of the proposed method.

Results

The presented formulation is tested in a multiphase porous media flow simulation in heterogeneous 2D test case. For the forward model, ICFERST is used (Jackson et al. (2015); Gomes et al. (2017); Salinas et al. (2017)).

To help the reader, a summary of the multi-phase porous media flow equations are presented, for a more in depth description see Gomes et al. (2017). The saturation equation for an incompressible flow is as follows:

$$\phi \frac{\partial S_\alpha}{\partial t} + \nabla \cdot (\mathbf{u}_\alpha S_\alpha) = 0, \quad (21)$$

in which ϕ is the porosity, t is time, \mathbf{u}_α and S_α are the velocity and saturation of phase α .

Darcy’s equation is as follows:

$$\mu_\alpha S_\alpha (\mathcal{K}_{r_\alpha} \mathbf{K})^{-1} \mathbf{u}_\alpha = -\nabla p + \mathbf{s}_{u_\alpha}, \quad (22)$$

where p is the global pressure of the system, \mathbf{s}_{u_α} is a source term; here no sources are considered. \mathbf{K} is the permeability tensor and \mathcal{K}_{r_α} and μ_α are the relative permeability and viscosity of phase α respectively.

The final equation is the summation constraint:

$$\sum_{\alpha=1}^n S_\alpha = 1, \quad (23)$$

n being the number of phases. The relative permeability is calculated using the Brooks-Corey model (Brooks and Corey, 1964):

$$k_{rw}(S_w) = \left(\frac{S_w - S_{wirr}}{1 - S_{wirr} - S_{nwr}} \right)^{n_w}, \quad (24)$$

$$k_{rnw}(S_{nw}) = \left(\frac{S_{nw} - S_{nwr}}{1 - S_{wirr} - S_{nwr}} \right)^{n_{nw}}, \quad (25)$$

where S_{nwr} is the irreducible non-wetting phase saturation and S_{wirr} is the irreducible wetting phase saturation; n_w and n_{nw} are the exponents for the wetting and non-wetting phases respectively.

Algorithm 1 Calculate $\hat{\mathbf{g}}$ using method in section

```

1: !! Run unperturbed forward model
2:  $\bar{\mathbf{m}} = \text{read\_in\_initial\_condition}()$ 
3:  $\bar{\boldsymbol{\psi}} = \text{run\_forward\_model}(\bar{\mathbf{m}})$ 
4:  $\bar{\mathbf{F}} = \text{calculate\_F}(\bar{\boldsymbol{\psi}})$ 
5:
6: !! Initialise sensitivity map vector
7:  $\hat{\mathbf{g}}^0 = \mathbf{1}$ 
8:
9: for ensemble  $e = 1$  to  $\mathcal{E}$  do
10:    $\Delta^e \mathbf{m} = \text{get\_perturbation}(\hat{\mathbf{g}}^0)$ 
11:    ${}^e \mathbf{m} = \text{get\_perturbed\_initial\_condition}(\Delta^e \mathbf{m}, \bar{\mathbf{m}})$ 
12:    ${}^e \boldsymbol{\psi} = \text{run\_forward\_model}({}^e \mathbf{m})$ 
13:    ${}^e \mathbf{F} = \text{calculate\_F}({}^e \boldsymbol{\psi})$ 
14:
15:   !! Calculate sensitivity map for time level 0 based on ensembles 1 to e
16:    $\mathbf{M}^0 = \text{calculate\_d}\boldsymbol{\psi}\text{dm}({}^1 \boldsymbol{\psi}^0, {}^2 \boldsymbol{\psi}^0, \dots, {}^e \boldsymbol{\psi}^0)$ 
17:    $\frac{d\mathbf{F}}{d\mathbf{m}} = \text{calculate\_dFdm}({}^1 \mathbf{F}, {}^2 \mathbf{F}, \dots, {}^e \mathbf{F})$ 
18:    $\hat{\mathbf{g}}^0 = \text{calculate\_Importance\_Map}(\mathbf{M}^0, \frac{d\mathbf{F}}{d\mathbf{m}})$ 
19: end for
20:
21: !! Calculate the sensitivity map at each desired time level
22: !! ... based on all  $\mathcal{E}$  ensembles
23:  $\frac{d\mathbf{F}}{d\mathbf{m}} = \text{calculate\_dFdm}({}^1 \mathbf{F}, {}^2 \mathbf{F}, \dots, {}^e \mathbf{F})$ 
24: for each time level  $n$  do
25:    $\mathbf{M}^n = \text{calculate\_d}\boldsymbol{\psi}\text{dm}({}^1 \boldsymbol{\psi}^n, {}^2 \boldsymbol{\psi}^n, \dots, {}^e \boldsymbol{\psi}^n)$ 
26:    $\hat{\mathbf{g}}^n = \text{calculate\_Sensitivity\_Map}(\mathbf{M}^n, \frac{d\mathbf{F}}{d\mathbf{m}})$ 
27: end for

```

2D porous media test case

The porous media model considered here consists of a square reservoir ($K_{out} = 1$ dimensionless permeability units) with a low permeable inclusion-square ($K_{out} = 10^{-5}$ dimensionless permeability units); the porosity of the domain is homogeneous and equal to 0.2. Initially the domain is saturated by the non-wetting phase with an initial saturation of $1 - S_{wirr}$. The wetting phase is injected from the left-hand side at a rate of 1 dimensionless velocity units, displacing the wetting and non-wetting phases to the right-hand-side. A viscosity ratio of 1 is considered. The time-step used is 0.001 and the final time is 0.1.

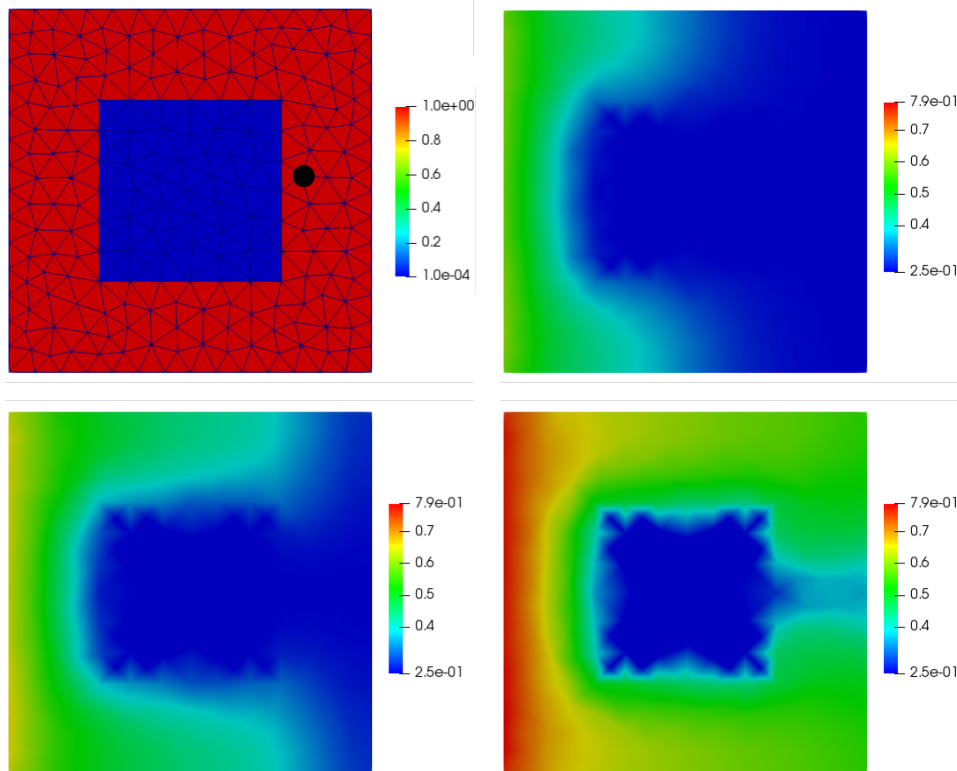


Figure 1 Top-left shows the mesh used for the experiments, the permeability map and the point of interest. The other figures shows the saturation of the injected wetting phase at three different stages. The fluids flow preferentially around the internal low permeable object.).

Figure 1 shows the mesh, the permeability map, the point of interest, towards which the sensitivity map is calculated and the forward simulation at three different time-levels. These figures illustrate how the fluid flows preferentially around the low permeable inclusion, as expected. Two sets of experiments are carried out in which 40 ensembles are considered in both cases. In one set we use just one single time-window and in the second set 4 time-windows of 5 time-levels is considered. Figure 2 shows the results of the first set. It can be seen how both test cases provide the expected results, showing that the area of interest goes around the low permeable inclusion. Comparing with the case using 4 time-windows, the results are much better defined with much fewer oscillations in the results.

Conclusions

We present a demonstration of goal-based sensitivity maps (Heaney et al., 2018) applied to a porous media flow problem. The approach uses an ensemble-based method which can concentrate perturbations in the area in which they will have most influence on the functional. Time windows are shown to improve the results, producing less fluctuating sensitivity maps.

Acknowledgements

The authors are grateful for the support of the EPSRC through: the Smart-GeoWells Newton grant (P65437); Managing Air for Green Inner Cities (MAGIC, EP/ N010221/1); the multi-phase flow programme grant (MEMPHIS, EP/ K003976/1); multi-phase flow for subsea applications (MUFFINS, EP/

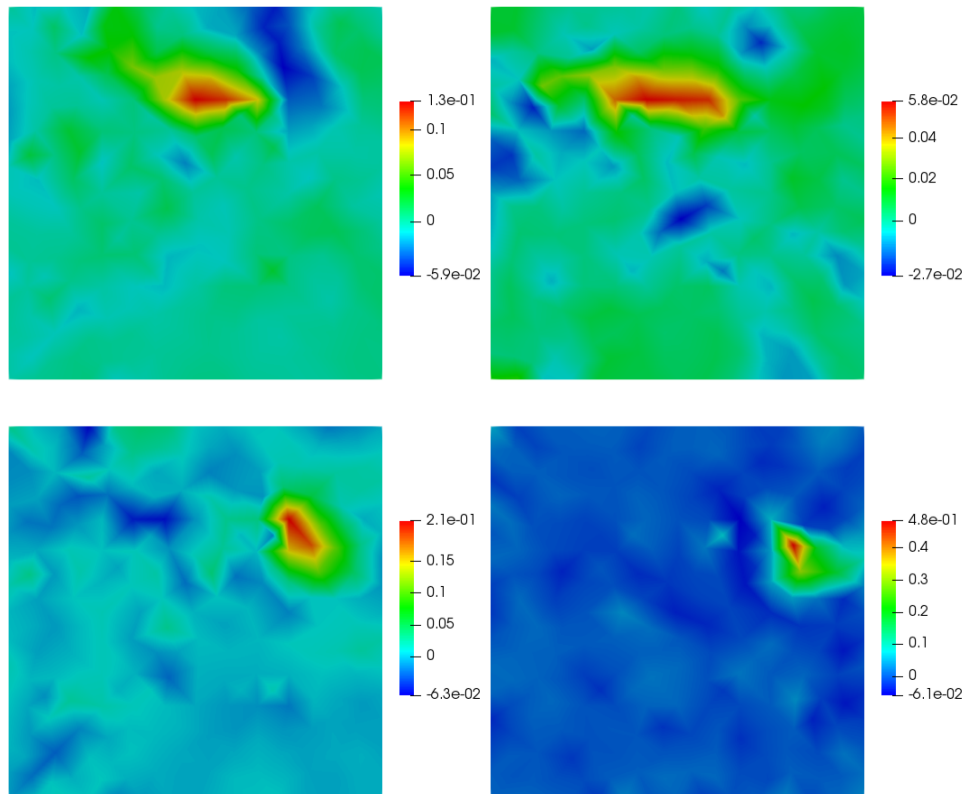


Figure 2 Left column shows the results using just one single time-window. Right column using 4 time-windows. Top and bottom figures show the sensitivity map at two different time-levels. The results using time-windows are more clearly defined than using just one.).

P033148/1); and also funding from the European Union Seventh Frame work Programme under grant agreement No.603663 for the research project Preparing for Extreme And Rare events in coastal regions (PEARL).

References

- Attia, A. [2016] *Advanced Sampling Methods for Solving Large-Scale Inverse Problems*. Ph.D. thesis, Department of Computer Science, Virginia Polytechnic Institute and State University.
- Blum, J., Le Dimet, F.X. and Navon, I.M. [2009] Data Assimilation for Geophysical Fluids. In: Temam, R.M. and Tribbia, J.J. (Eds.) *Special Volume: Computational Methods for the Atmosphere and the Oceans, Handbook of Numerical Analysis*, 14, Elsevier, 385–441.
- Brooks, R.H. and Corey, A.T. [1964] Hydraulic properties of porous media. In: *Hydrology Papers*.
- Cacuci, D.G. [2015] Second-order adjoint sensitivity analysis methodology (2nd-ASAM) for computing exactly and efficiently first- and second-order sensitivities in large-scale linear systems: I. Computational methodology. *Journal of Computational Physics*, **284**, 687–699.
- Cacuci, D.G., Ionescu-Bujor, M. and Navon, I.M. [2005] *Sensitivity and Uncertainty Analysis, Volume II: Applications to Large-Scale Systems*. CRC Press.
- Che, Z., Fang, F., Percival, J., Pain, C.C., Matar, O. and Navon, I.M. [2014] An ensemble method for sensor optimisation applied to falling liquid films. *International Journal of Multiphase Flow*, **67**, 153–161.
- Gomes, J.L.M.A., Pavlidis, D., Salinas, P., Xie, Z., Percival, J.R., Melnikova, Y., Pain, C.C. and Jackson, M.D. [2017] A Force-Balanced Control Volume Finite Element Method for Multiphase Porous Media Flow Modelling. *International Journal for Numerical Methods in Fluids*, **83**, 431–445.
- Heaney, C.E., Salinas, P., Fang, F., Pain, C.C. and Navon, I.M. [2018] Goal-based sensitivity maps using time windows and ensemble perturbations. *ArXiv e-prints*.
- Hossen, M.J., Navon, I.M. and Daescu, D.N. [2012] Effect of random perturbations on adaptive observation techniques. *International Journal for Numerical Methods in Fluids*, **69**(1), 110–123.

- Ionescu-Bujor, M. and Cacuci, D.G. [2004] A Comparative Review of Sensitivity and Uncertainty Analysis of Large-Scale Systems-I: Deterministic Methods. *Nuclear Science and Engineering*, **147**(3), 189–203.
- Jackson, M.D., Percival, J.R., Mostaghimi, P., Tollit, B.S., Pavlidis, D., Pain, C.C., Gomes, J.L.M.A., El-Sheikh, A.H., Salinas, P., Muggeridge, A.H. and Blunt, M.J. [2015] Reservoir Modeling for Flow Simulation by Use of Surfaces, Adaptive Unstructured Meshes, and an Overlapping-Control-Volume Finite-Element Method. *SPE Reservoir Evaluation & Engineering*, **18**.
- Keller, J.D., Hense, A., Kornblueh, L. and Rhodin, A. [2010] On the Orthogonalization of Bred Vectors. *Weather and Forecasting*, **25**, 1219–1234.
- Leroux, R., Chatellier, L. and David, L. [2018] Time-resolved flow reconstruction with indirect measurements using regression models and Kalman filtered POD ROM. *Experiments in Fluids*, **59**, 1–27.
- Liu, J. and Kalnay, E. [2008] Estimating observation impact without adjoint model in an ensemble Kalman filter. *Quarterly Journal of the Royal Meteorological Society*, **134**(634), 1327–1335.
- Maday, Y. and Taddei, T. [2017] Adaptive PBDW approach to state estimation: noisy observations; user-defined update spaces. *ArXiv e-prints*.
- Merton, S.R., Buchan, A.G., Pain, C.C. and Smedley-Stevenson, R.P. [2013] An adjoint-based method for improving computational estimates of a functional obtained from the solution of the Boltzmann Transport Equation. *Annals of Nuclear Energy*, **54**, 1–10.
- Merton, S.R., Smedley-Stevenson, R.P., Pain, C.C. and Buchan, A.G. [2014] Adjoint eigenvalue correction for elliptic and hyperbolic neutron transport problems. *Progress in Nuclear Energy*, **76**, 1–16.
- Nerger, L., Schulte, S. and Bunse-Gerstner, A. [2014] On the influence of model nonlinearity and localization on ensemble Kalman smoothing. *Quarterly Journal of the Royal Meteorological Society*, **140**, 2249–2259.
- Power, P.W., Piggott, M.D., Fang, F., Gorman, G.J., Pain, C.C., Marshall, D.P., Goddard, A.J.H. and Navon, I.M. [2006] Adjoint goal-based error norms for adaptive mesh ocean modelling. *Ocean Modelling*, **15**(1), 3–38.
- Salinas, P., Pavlidis, D., Xie, Z., Jacquemyn, C., Melnikova, Y., Pain, C.C. and Jackson, M.D. [2017] Improving the Robustness of the Control Volume Finite Element Method with Application to Multiphase Porous Media Flow. *International Journal for Numerical Methods in Fluids*, **85**, 235–246.
- Shah, A.J. [2017] Methods for Data Assimilation for the Purpose of Forecasting in the Gulf of Cambay (Khambhat). *IJSRSET*, **3**, 224–228.
- Shapiro, R. [1970] Smoothing, Filtering and Boundary Effects. *Review of Geophysics and Space Physics*, **8**, 359–387.
- Wang, Z., Navon, I.M., Le Dimet, F.X. and Zou, X. [1992] The second order adjoint analysis: Theory and applications. *Meteorology and Atmospheric Physics*, **50**(1), 3–20.